
Functional Ensemble Distillation

Coby Penso

Bar-Ilan University, Israel
coby.penso24@gmail.com

Idan Achituve

Bar-Ilan University, Israel
idan.achituve@biu.ac.il

Ethan Fetaya

Bar-Ilan University, Israel
ethan.fetaya@biu.ac.il

Abstract

Bayesian models have many desirable properties, most notable is their ability to generalize from limited data and to properly estimate the uncertainty in their predictions. However, these benefits come at a steep computational cost as Bayesian inference, in most cases, is computationally intractable. One popular approach to alleviate this problem is using a Monte-Carlo estimation with an ensemble of models sampled from the posterior. However, this approach still comes at a significant computational cost, as one needs to store and run multiple models at test time. In this work, we investigate how to best distill an ensemble’s predictions using an efficient model. First, we argue that current approaches that simply return distribution over predictions cannot compute important properties, such as the covariance between predictions, which can be valuable for further processing. Second, in many limited data settings, all ensemble members achieve nearly zero training loss, namely, they produce near-identical predictions on the training set which results in sub-optimal distilled models. To address both problems, we propose a novel and general distillation approach, named Functional Ensemble Distillation (FED), and we investigate how to best distill an ensemble in this setting. We find that learning the distilled model via a simple augmentation scheme in the form of mixup augmentation [42] significantly boosts the performance. We evaluated our method on several tasks and showed that it achieves superior results in both accuracy and uncertainty estimation compared to current approaches.

1 Introduction

In parametric Bayesian inference the output is a distribution over model parameters, known as the posterior distribution. This is in contrast to standard approaches which return a single model. At test time one needs to marginalize over all models according to the posterior distribution to make a prediction. The action of averaging over multiple models allows Bayesian approaches to perform well with limited data [1, 2, 26, 33, 41] and properly estimate uncertainties [16, 17, 33]. The downside is that in most cases Bayesian inference is intractable and even methods for approximate inference may be costly. This is especially true for Bayesian neural networks (BNNs), as the dimension of the parameter space for common neural networks is very large [4, 14].

Two main approaches exist for efficient Bayesian inference. The first is variational inference, where we fit a simple distribution, usually a Gaussian with diagonal covariance, to the posterior. While this can be done efficiently in some cases [19], it is more prone to over-fitting as the variational distribution might cover only a small part of the posterior. A second approach is Monte-Carlo (MC) estimation where we sample M models from the posterior using an approximate sampling algorithm, e.g. Markov Chain Monte-Carlo (MCMC), and estimate the mean prediction by the average over the predictions of the M models. While this can better capture the diversity of the posterior, it requires storing and running M models instead of one. One important question that will be the focus of this work is how to maintain the benefits of the Bayesian approach while reducing the computational overhead. It is also important to note that using an ensemble of M models is commonly used outside

of Bayesian settings, e.g. bagging [3], so this line of work has wider implications. Our focus, however, will be in the low-data regime where Bayesian methods are most impactful.

We propose an ensemble distillation [15, 25] method that mimics an ensemble of models using a lightweight model. Current approaches mainly consider classification where a single prediction is a probability vector, the distilled model then outputs parameters of a Dirichlet distribution that should fit the ensemble predictions. Our approach, which we call Functional Ensemble Distillation (FED), on the other hand tries to learn a distribution over functions by transferring the randomness to ϵ , a noise variable that is sampled from a fixed distribution. We designed our model with two requirements in mind. First, it should be fast to run during test time. This is achieved by being able to run with multiple ϵ values in parallel. Second, the distribution of predictions from our model should match the distribution of predictions from the posterior. This approach allows us more flexibility as it is not limited to classification tasks and to the Dirichlet distribution, unlike most previous approaches. Furthermore, our method allows us to compute covariance between predictions which can be useful for further downstream tasks. Consider, for example, the task of object detection for autonomous vehicles. If two nearby detections are made with certain confidence then the probability that that area of space is occupied depends heavily on the correlation between these predictions.

Finally, we investigate how to properly distill from a model ensemble under severe overfitting. It is common for deep networks trained on small datasets such as CIFAR-10 [21] to reach almost perfect accuracy on the training set while still generalizing well to the test set. In these cases, the predictions of the models in the ensemble can vary considerably on the test set despite being almost identical on the training set. This means that distilling the ensemble on the training set will not capture the diversity between predictions which is the core component of ensemble methods. While some previous works tried to address this issue [25, 28], they either depended on additional unsupervised data that might not be readily available, e.g. medical imaging, or do not scale well. Here we propose a simple solution for this problem that works remarkably well - creating an auxiliary dataset using the mixup augmentation [42]. The mixup procedure generates data that is on the one hand distinct enough from the training set to allow our ensemble to produce diverse predictions, while on the other hand, being close enough to it so that models that were trained on it work well when applied to the original test data.

To conclude, we make the following novel contributions: (i) We propose a general-purpose and flexible method for ensemble distillation that captures well the predictive abilities and the diversity of the original ensemble; (ii) we propose a simple, fast, and scalable method for obtaining a diverse auxiliary dataset for training the distilled model without *any* new samples using the mixup augmentation; and (iii) we evaluated our method on several image benchmarks and showed that it obtains the best results in terms of accuracy and calibration compared to other ensemble distillation approaches.

2 Background

We first provide a brief introduction to the main components of our model. We use the following notations in the paper. We denote scalars with lower-case letters (e.g., x), and vectors with bold lower-case letters (e.g., \mathbf{x}). We assume we are given with a dataset \mathcal{D} of size N , $\mathcal{D} = \{(\mathbf{x}_i, y_i)\}_{i=1:N}$, where $\mathbf{x}_i \in \mathbb{R}^d$ are the training examples and y_i are the corresponding labels or targets.

2.1 Bayesian Inference

In Bayesian inference we are mainly interested in the posterior distribution $p(\theta|\mathcal{D}) \propto \prod_i p(y_i|\mathbf{x}_i, \theta)p(\theta)$, where θ denotes the parameters of the model (e.g., a NN). The posterior tells us how likely θ is given the observed data. When given a new data point \mathbf{x}_* we will use the entire posterior to calculate the predictive distribution using the rule $p(y_*|\mathbf{x}_*, \mathcal{D}) = \int p(y_*|\mathbf{x}_*, \theta)p(\theta|\mathcal{D})d\theta$. One intuition behind this is that when one has limited data, there are many distinct models that work well on the training set. By averaging over all the possible predictors the final prediction is supported by most of the “weight” in the posterior instead of by a single model. This also leads to better uncertainty estimation, as when many different models have different predictions the resulting average prediction is dispersed and uncertain.

In practice, besides a few notable exceptions, computing this integral is computationally intractable. One popular approximate inference solution is Monte-Carlo (MC) estimation. Namely, we estimate

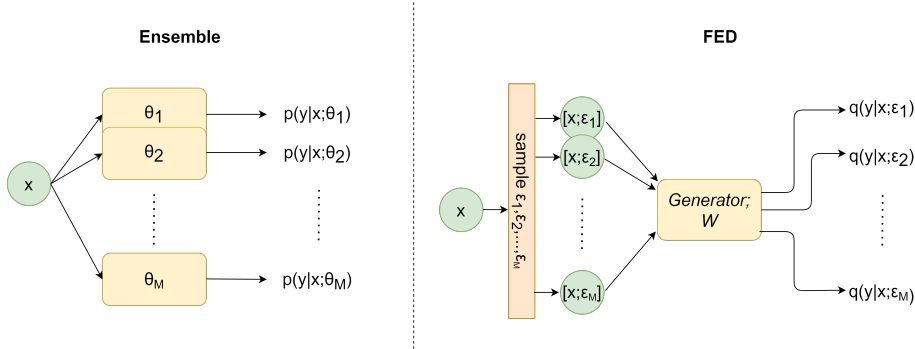


Figure 1: (1) Ensemble Forward pass pipeline. (2) FED Forward pass pipeline.

$p(y_*|\mathbf{x}_*, \mathcal{D}) \approx \frac{1}{M} \sum_{m=1}^M p(y_*|\mathbf{x}_*, \theta_m)$, where θ_m are (approximate) samples from the posterior $p(\theta|\mathcal{D})$. Obtaining such samples can be achieved in various ways such as MCMC methods [29, 37, 43]. One problem with this approach is that it requires storing and running multiple models to obtain the predictive distribution. This may be impractical in many situations such as when making predictions in low resource environments or in real-time systems.

2.2 Maximum Mean Discrepancy

A big question in machine learning and statistics is how to measure distances between distributions, specifically without access to the density function and with only access to samples. One well known measure is the Maximum Mean Discrepancy (MMD) [36] that was used as an objective to successfully train generative models [22, 23]. Given a family of functions \mathcal{F} the MMD score between two distributions p, q is defined as $MMD(p, q) = \sup_{f \in \mathcal{F}} |\mathbb{E}_{\mathbf{x} \sim p}[f(\mathbf{x})] - \mathbb{E}_{\mathbf{x} \sim q}[f(\mathbf{x})]|$. A specific case in which the MMD has a closed form formula is when \mathcal{F} is the unit sphere in a reproducing kernel Hilbert space (RKHS) defined by a kernel function k [12]. In that case we have

$$MMD(p, q)^2 = \mathbb{E}_{\mathbf{x}, \mathbf{x}' \sim p}[k(\mathbf{x}, \mathbf{x}')] - 2\mathbb{E}_{\mathbf{x} \sim p, \mathbf{y} \sim q}[k(\mathbf{x}, \mathbf{y})] + \mathbb{E}_{\mathbf{y}, \mathbf{y}' \sim q}[k(\mathbf{y}, \mathbf{y}')], \quad (1)$$

which we estimate by Monte-Carlo means.

2.3 Mixup Training Procedure

The mixup [42] training procedure is based on the Vicinal Risk Minimization principle [6]. The main idea is to enlarge the training set by sampling points in the neighborhood of the given data. [42] proposed a simple way to achieve this goal by sampling along the line which connects two data points from the training set. Let $(\mathbf{x}_i, y_i), (\mathbf{x}_j, y_j)$ be two training examples, one can generate a new data point $(\tilde{\mathbf{x}}, \tilde{y})$ by taking their convex combination: $\tilde{\mathbf{x}} = \lambda \mathbf{x}_i + (1 - \lambda) \mathbf{x}_j$, and $\tilde{y} = \lambda y_i + (1 - \lambda) y_j$, where λ is drawn from a Beta distribution with some fixed parameters. Now, standard loss functions, such as the cross entropy loss, can be used on $(\tilde{\mathbf{x}}, \tilde{y})$.

3 Related Work

Several previous studies proposed approaches to distill an ensemble of models into a single fast model. Early approaches [5, 15, 20, 31, 39] focused on capturing only the mean behaviour of the ensemble but did not capture the diversity in it, which may be crucial for uncertainty estimation. For example, in [5] it was first shown that a single network can learn the knowledge of a large ensemble of networks. In [15] a distilled model is learned using a convex combination of the ensemble predictions in addition to the standard cross-entropy loss. And, in [20] a student networks is learned online from a teacher that is trained via MCMC training procedures.

More recent studies proposed alternatives for capturing the diversity as well. Ensemble Distribution Distillation (EnDD) [25] was the first to propose such an approach. EnDD builds on the method in [24] which tries to emulate the behaviour of an ensemble with a Dirichlet distribution parameterized by a NN. To handle the fact that the ensemble predictions are over-confident and have low diversity

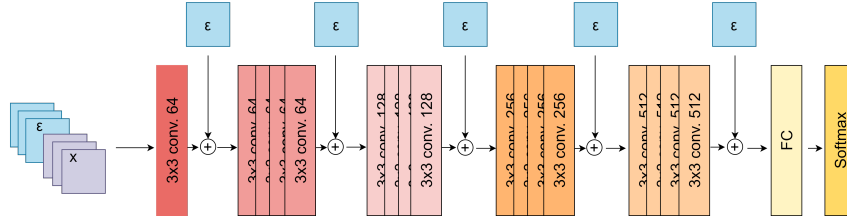


Figure 2: Generator architecture. First, we concatenate 3 random Gaussian channels to the input. Second, add Gaussian noise to intermediate features along the ResNet-18 architecture.

on the training set, they proposed to use an unsupervised auxiliary dataset for training the distilled model, and to perform temperature annealing. Similarly, [9] also makes the assumption that the predictive distribution follows a Dirichlet distribution. They fit the output to the teacher network by two separate networks, one that learns the predicted class probabilities, i.e. the Dirichlet mean, and another that learns the confidence, i.e. the Dirichlet concentration. Both [25, 9] are suitable for classification tasks only and assume a Dirichlet distribution behaviour which may be too restrictive. We argue that a more general solution for the distillation of ensembles is needed.

A different line of work [35, 28] generalizes the method in [15] by distilling the ensemble members to task heads in a one-to-one fashion. In [35] the distilled model is partitioned into two parts, a shared “body” and a member-specific “head”, one per ensemble member. Each head is trained to copy the prediction of an ensemble member using the standard cross-entropy loss function. In [28] the authors propose to use BatchEnsemble [38] for weight sharing. They increase the diversity in the ensemble predictions on the training set by randomly perturbing the training data based on three techniques: Gaussian, Output diversified sampling (ODS) [34], and ConfODS. The ODS perturbations are similar to adversarial perturbations and need to be computed at every iteration. This imposes a computational overhead which renders a slow training process and inability to easily handle large ensembles, unlike our proposed method.

4 Our Method

We take a similar approach to [9, 25] where we treat the ensemble distillation as a conditional generative model. Given an input \mathbf{x} and a sampled model parameters θ we get a distribution $p(y|\mathbf{x}, \theta)$, so for a given \mathbf{x} we can push-forward the posterior distribution over weights to a distribution over distributions over y . While this was done in [9, 25], there are several limitations with these approaches. First, they use a Dirichlet distribution to model this distribution over distributions, which is limited to classification and has limited expressive power. Second, given two inputs $\mathbf{x}_1, \mathbf{x}_2$ the correlation between their predictions cannot be calculated by the distilled Dirichlet distributions. This can be very important as one of the main motivations for Bayesian inference is its ability to measure uncertainty. In many applications, e.g. autonomous driving, the output predictions are fed into a planning module that needs uncertainty estimation to make the optimal plan.

Our approach is to model a distribution over functions that both have low memory requirements and that we can parallelize to get multiple predictions quickly. We do this by training a generator neural network with parameters \mathbf{w} and added random noise ϵ . The noise can be added, for example, as an additional channels to the input or hidden layers. Our goal is to train the generator network so that the distribution over $q(y|\mathbf{x}, \mathbf{w}, \epsilon)$ for $\epsilon \sim p(\epsilon)$ will match that of $p(y|\mathbf{x}, \theta)$ for $\theta \sim p(\theta|\mathcal{D})$. Namely, each draw of ϵ corresponds to a draw from the posterior. By using this design we get a similar memory cost to a standard single network and we can parallelize easily as all the linear operations are shared. Computationally it is equivalent to running a single model on a batch instead of a single input. An illustration of our method is presented in Figure 1. We further show in the appendix that for a wide range of batch sizes the runtime of our model scales approximately as $1 + (\# \text{ of } \epsilon \text{ samples})/35$ resulting in a considerable speedup. Since we now have a distribution over functions, we call our method *Functional Ensemble Distillation (FED)*.

We now present our training objective for the generator $g_{\mathbf{w}}$. Given an ensemble member θ_j and a batch of B examples, we consider the vectors of predicted probabilities (one per example) as

Algorithm 1 Generator training

```
1: input: Predictions of the ensemble on our distillation dataset:  $\{\mathbf{x}_i, \{\mathbf{p}_i^j\}_{j=1:M}\}_{i=1:N}$   
   #  $N$  number of data points,  $M$  ensemble predictions  
2: Initialize Generator  $g_w$   
3: while not converged do  
4:   Sample batch of inputs and model predictions  $\{\mathbf{x}_i, \{\mathbf{p}_i^j\}_{j=1:M}\}_{i=1:B}$   
5:   Sample  $M$  latent variables -  $\epsilon \sim \mathcal{N}(0, \sigma^2)$   
6:    $\mathbf{q}_i^j = g_w(\mathbf{x}_i, \epsilon_j)$   
7:    $\hat{\mathbf{q}}^j = \text{concat}(\mathbf{q}_1^j, \dots, \mathbf{q}_B^j)$   
8:    $\hat{\mathbf{p}}^j = \text{concat}(\mathbf{p}_1^j, \dots, \mathbf{p}_B^j)$   
9:    $\mathcal{L} = \widehat{MMD}^2(\{\hat{\mathbf{p}}^j\}_{j=1:M}, \{\hat{\mathbf{q}}^j\}_{j=1:M})$   
10:   $\mathbf{w} \leftarrow \mathbf{w} - \nabla_{\mathbf{w}} \mathcal{L}$   
11: end while  
12: return  $g_w$ 
```

features representing the function parameterized by θ_j . Denote by $\mathbf{p}_i^j = p(y_i|\mathbf{x}_i, \theta_j)$ the predictive likelihood for the i^{th} example by the j^{th} function. We represent the function parameterized by θ_j by concatenating these vectors to form a feature vector $\hat{\mathbf{p}}^j = \text{concat}(\mathbf{p}_1^j, \dots, \mathbf{p}_B^j)$. We repeat this process for our generator network (only that now each ϵ_i represents a function) and in a similar fashion, we obtain a representation $\hat{\mathbf{q}}^j = \text{concat}(\mathbf{q}_1^j, \dots, \mathbf{q}_B^j)$ using the same batch. The same process is applied to every member of the ensemble. Now we use the MMD objective presented in Section 2.2 to score the difference between distribution over functions, using a simple kernel over these functions' representations. More formally, the MMD objective given a batch of examples is:

$$\widehat{MMD}^2(\{\hat{\mathbf{p}}^j\}_{j=1:M}, \{\hat{\mathbf{q}}^j\}_{j=1:M}) = \frac{1}{M^2} \sum_{i,j} (k(\hat{\mathbf{p}}^i, \hat{\mathbf{p}}^j) + k(\hat{\mathbf{q}}^i, \hat{\mathbf{q}}^j) - 2k(\hat{\mathbf{p}}^i, \hat{\mathbf{q}}^j)). \quad (2)$$

We present our method in Algorithm 1. In our experiments, we used standard convolutional neural networks where we concatenated 3 random Gaussian channels to the input channels and we add Gaussian noise to intermediate features across the network. We evaluated several options for inserting noise into the generative model and noticed that to learn sufficient diversity, enough noise has to be inserted; otherwise, the generator's diversity suffers and collapses to a nearly deterministic model. We also found it best to set the noise STD to be a learnable parameter (one parameter per input noise layer). See an illustration with ResNet18 in Figure 2. Regarding the limitations of our approach, we note that while the run-time is much faster than running the full ensemble, there is still a non-negligible overhead compared to a single model.

4.1 Auxiliary Dataset

One problem with distilling ensemble models is that the predictions of the ensemble members on the training set have a much higher agreement compared to the test set (as can be seen in Table 1). Practically this means that distillation of the ensemble predictions on the training set can lead to a degenerate solution that returns in most cases the same predictions. This leads to worse performance in both accuracy and calibration compared to the original ensemble.

In [25] the authors address this by using an auxiliary unsupervised dataset, as we can get diverse ensemble predictions on this dataset and use it to train our distilled model. While this solution performs quite well, in several applications having access to an additional unsupervised dataset is not trivial. One example is medical imaging [8], where even unsupervised data requires access to expensive machinery and data that is not readily shared due to privacy concerns. Another example is learning from ancient texts [11] where digitized data, labeled or unlabeled, is scarce. We argue that these problems in which the data is limited are exactly the problems where Bayesian methods can make the most impact. Therefore, having a method that works on these types of data is of great importance.

This leads us to seek a solution that does not require any additional data, even if it is unsupervised. We investigated several solutions (see Section 5.4) and found one simple solution that worked surprisingly well, the mixup augmentation. The predictions on the mixup data are more diverse allowing us to distill from data that more closely resembles the test data. Another important property of the mixup augmentation is that models trained on it transfer well to real images. This is in contrast to other alternatives that we explored, such as generating an auxiliary dataset using a generative adversarial network (GAN), that did not transfer well.

To summarize we generate a synthetic, unlabeled, dataset from the original training set (that was used to train the original ensemble) using the mixup augmentation. We then train our generator network using the predictions of the original ensemble on this dataset, see Algorithm 1. In Table 3, we show that indeed the ensemble classifier generates a more diverse set of predictions on the mixup dataset compared to the actual training set.

5 Experiments

We evaluated FED against baseline methods on different datasets and using different metrics. We present here the results of the models using the hyperparameters with the best accuracy on the validation set. As a result, for some models the diversity can be improved at the expense of lower accuracy. We also provide our code for reproducibility - https://github.com/cobypenso/functional_ensemble_distillation.

Datasets. We evaluated all methods on CIFAR-10, CIFAR-100 [21], and STL-10 [7] datasets. STL-10 and CIFAR-100 are considered more challenging, the former has a relatively small amount of labeled training data (10 classes with 500 labeled examples per class), and the latter has more categories. For all datasets we use train/val/test split. The train/val split with a ratio 80%:20%.

Compared methods. We compare our method against the following baselines: (1) *EnDD* [25], Ensemble Distribution Distillation framework, trained with the same train data used to capture the ensemble. (2) *EnDD_{AUX}* [25], Ensemble Distribution Distillation framework, trained with the train data and an auxiliary dataset. For CIFAR-10, CIFAR-100 is the auxiliary dataset. For CIFAR-100, CIFAR-10 is the auxiliary dataset. For STL-10 we used the unlabeled data provided as part of this dataset. We stress that other methods do not have access to this data. (3) *DM* [28], this baseline comes in three variations, *Gaussian*, *ODS*, and *ConfODS*. (4) *AMT* [9], a method which also uses MMD as an objective. (5) *Hydra* [35], a weight sharing method based on [15].

Ensemble. We created the Bayesian ensemble (for distillation) by sampling from a posterior obtained with the Cyclic Stochastic Gradient Hamiltonian Monte Carlo (cSGHMC) method [43]. Overall we sampled 120 models. In addition, we show experimented with different ensemble methods and their implications on the distillation. The architecture we choose for the models in the ensemble is ResNet18 with Group Norm [40] and Weight Standardization [32]. We did not use Batch normalization since it breaks the IID assumption used in Bayesian Inference [16].

We note that sampling from the posterior with cSGHMC, instead of SGD, slightly improves the ensemble diversity on the training set. If our ensemble was sampled using SGD with different seeds the effect of mixup would be even more pronounced.

Training setup. For the baselines, we follow the training strategies suggested in the papers and their code if available, while performing an extra hyperparameter search when training on datasets which did not cover in the original papers, mainly CIFAR-100 and STL-10. For our method, we performed a standard training procedure with Adam optimizer [18], a learning rate scheduler with fixed milestones at epochs {35, 45, 55, 70, 80}, and a hyperparameter search done over a held-out validation set.

Objective and Kernel choice. We trained our model using the MMD objective while considering various kernels. Specifically, we examined Linear kernel, RBF kernels, and a mixture of RBF kernels. For the RBF kernel, we considered different values of length scales, as we saw that it had a considerable effect on the results. For CIFAR-10, a mixture of RBF kernels with {2, 10, 20, 50} length scales had the best results. For CIFAR-100, the length scales are {10, 15, 20, 50}, and for STL-10 a length scale of 50 works best.

Distilled Model. We distilled using a similar ResNet18 with Group Norm and Weight Standardization architecture as the ensemble models. Thus, essentially trying to distill a 120 models ensemble into

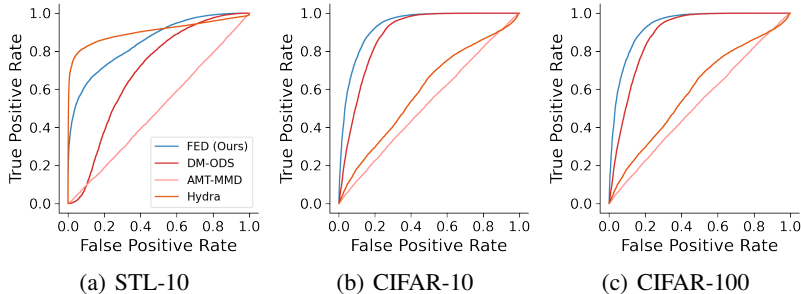


Figure 3: Receiver operating characteristic (ROC) curve measuring the performance on in-distribution vs out-of-distribution data based on the mutual information. Best viewed in color.

a single model that has almost the same size as a member in the ensemble, i.e a $\sim 100\times$ memory improvement. Memory and Timing performance analysis can be found in the Appendix. For the noise sampled and fed into the generative model, we chose a simple Gaussian distribution, fed by concatenating it to the input, and by inserting it in intermediate places along the model. Specifically, for the concatenation part, 3 channels of noise and 3 channels of the input are stacked together. For the intermediate noise, the Gaussian noise was added to the features, instead of concatenation, in 5 different places, one after the first convolution layer and the other four after each Block in the ResNet-18 architecture (Figure 2). We found that setting the standard deviation of the noise to be a learnable parameter as part of the optimization, has a slight performance improvement.

Metrics. To evaluate our method, and other baselines, we define the agreement metric as the probability that two distinct elements of our ensemble predict the same label on the same input. In addition, we computed accuracy, and Expected Calibration Error (ECE) [13] reported in percentages. For the agreement metric, a close value to the original ensemble’s agreement is a good indication that we capture similar behavior.

5.1 Ensemble Analysis

Table 1: Ensemble analysis. Test accuracy, agreement & ECE (%) on STL-10, and CIFAR-10/100.

	STL-10			CIFAR-10			CIFAR-100		
	ACC (\uparrow)	AGREEMENT	ECE (\downarrow)	ACC (\uparrow)	AGREEMENT	ECE (\downarrow)	ACC (\uparrow)	AGREEMENT	ECE (\downarrow)
Train	100.0	98.23	2.99	99.97	91.85	6.38	99.95	97.53	4.15
Test	81.84	87.85	2.17	94.41	86.08	5.56	77.79	71.97	3.07
mixup	-	95.20	-	-	88.08	-	-	88.56	-

We first analyze the ensemble we sampled using cSGHMC. To evaluate the diversity between predictions we use the agreement metric. We computed accuracy, agreement and Expected Calibration Error (ECE) [13, 27] over the trainset and testset. We only show agreement on our suggested mixup auxiliary dataset, as it does not have discrete labels. We can see that the ensemble has almost perfect accuracy and very high agreement on the training set, with a considerable drop in both on the testset. In fact, for CIFAR-100 and STL-10, the ensemble has essentially no diversity over the training set, thus making the trainset inappropriate for the distillation task. The mixup agreement closes part of the gap between the train and test datasets.

5.2 Distillation

We now evaluate FED on learning multi-class classification tasks. While we are not limited to classification tasks, In the following experiment we compare our approach to the baselines described above. Results in Table 2 show that FED outperforms previous methods that do not use an auxiliary dataset by a large margin, especially on the more challenging STL-10 and CIFAR-100 datasets. This is true for both accuracy and ECE. It is interesting to note that while EnDD_{AUX} uses additional unlabeled examples from the training distribution (between $50k$ and $100k$), FED is on par and often outperforms this baseline across all metrics.

Table 2: Test accuracy, agreement & ECE (%) (\pm STD) on STL-10 and CIFAR-10/100. Note that the EnDD_{AUX} baseline uses additional unsupervised data. Each experiment was repeated 3 times.

	STL-10			CIFAR-10			CIFAR-100		
	ACC (\uparrow)	AGREEMENT	ECE (\downarrow)	ACC (\uparrow)	AGREEMENT	ECE (\downarrow)	ACC (\uparrow)	AGREEMENT	ECE (\downarrow)
Ensemble	81.84	87.85	2.17	94.41	86.08	5.56	77.79	71.97	3.07
EnDD _{AUX}	80.78\pm.00	99.98 \pm .00	1.20\pm.00	91.05 \pm 1.3	100.0 \pm .00	5.63 \pm 1.0	70.68 \pm .00	100.0 \pm .00	21.40 \pm .00
EnDD	73.45 \pm 1.1	99.88 \pm .02	10.62 \pm 1.2	91.01 \pm .70	99.99 \pm .00	6.39 \pm .81	71.16 \pm .00	100.0 \pm .00	14.51 \pm .00
DM _{Gaussian}	74.21 \pm .13	86.63\pm3.4	15.17 \pm .58	90.27 \pm 1.5	95.88 \pm 1.7	2.48 \pm .94	72.44 \pm .19	85.97\pm.81	4.63 \pm 1.0
DM _{ODS}	73.90 \pm .65	86.72 \pm 4.3	15.32 \pm .88	89.35 \pm 2.7	95.51 \pm 1.7	2.65 \pm 1.2	71.85 \pm .36	87.90 \pm 4.1	4.47 \pm 1.0
DM _{ConjODS}	73.26 \pm 2.2	86.67 \pm 2.7	14.52 \pm 3.1	89.55 \pm 2.3	95.49 \pm 2.3	2.59 \pm .29	72.33 \pm .54	88.73 \pm 4.7	5.33 \pm 1.1
AMT _{MMD}	54.36 \pm .78	11.31 \pm .08	38.97 \pm .68	83.81 \pm .56	12.95 \pm .08	64.00 \pm .63	N/A \pm N/A	N/A \pm N/A	N/A \pm N/A
Hydra	75.74 \pm 1.6	93.40 \pm .26	30.68 \pm 3.3	91.07 \pm 1.8	94.60 \pm .62	5.39 \pm .61	69.56 \pm .11	93.80 \pm .46	29.84 \pm 1.0
FED (Ours)	80.61 \pm .36	97.18 \pm .06	3.41 \pm .94	93.61 \pm .06	93.34 \pm .34	0.66 \pm .10	74.48 \pm .10	87.82 \pm .60	1.64 \pm .17

We also show results for out-of-distribution (OOD) detection in Figure 3 using ROC curves (EnDD was excluded due to poor performance), To score the examples we used the knowledge uncertainty which is obtained by subtracting the aleatoric uncertainty from the total uncertainty [10, 25]. We used SVHN [30] as OOD data. See appendix for more details. From the figure, FED generally outperforms all baselines here as well.

5.3 Mixup Augmentation as Auxiliary Dataset

Table 3: Ablation - EnDD vs Fed with and without mixup. Test accuracy, agreement & ECE (%) on STL-10, CIFAR-10, and CIFAR-100.

	STL-10			CIFAR-10			CIFAR-100		
	ACC (\uparrow)	AGREEMENT	ECE (\downarrow)	ACC (\uparrow)	AGREEMENT	ECE (\downarrow)	ACC (\uparrow)	AGREEMENT	ECE (\downarrow)
EnDD	72.23	99.89	11.96	90.35	100.0	6.80	71.16	100.0	14.51
EnDD + mixup	78.40	99.99	7.68	90.83	100.0	5.74	68.78	100.0	15.86
FED	65.06	97.18	5.00	92.58	99.16	1.92	68.34	97.58	9.61
FED + mixup	80.94	97.16	2.55	93.68	93.71	0.78	74.56	88.20	2.07

As an ablation study, we would like to understand the separate effects of the mixup augmentation and our FED approach. Thus, we show results for both FED and EnDD trained on the training set and on the mixup dataset as the auxiliary dataset. Results are detailed in Table 3. We show that for our method the mixup adds a significant boost to performance, and also for EnDD on two out of three datasets. We also see that even when EnDD is trained with mixup, our approach returns better accuracy, ECE and also has greater diversity. We suspect that this is due to the limited expressive power of the Dirichlet distribution. Additional experiments in the Appendix show that at least part of the lack of diversity can be attributed to the Dirichlet distribution.

5.4 Alternatives for Learning Distilled Model Without Auxiliary Dataset

In this section, we explore an additional attempt to distill the ensemble, this time without access to additional data. This approach was inspired by the Out-Of-Bag (OOB) estimate in bagging. In bagging each model is trained only on a random subset of the training set and the OOB estimate is done by averaging the predictions of all models on those data points that they were not trained on and returning their score (which we refer to as held-out datasets). Using this approach, we can train each member in the ensemble on part of the dataset, and use for distillation only the ensemble members’ predictions on the data points that they were not trained on. As an example, consider a single datapoint x which is on the held-out dataset for model m_1 , but is part of the trainset for model m_2 . To train the distillation model, the ensemble uses only the predictions of model m_1 , but does not use those of model m_2 to get the overall output for x . We experimented with two different partitions for held-out datasets: K-fold and bagging.

In K-Fold we first split the data into $K = 10$ folds, $\mathcal{D}_1, \dots, \mathcal{D}_{10}$. For each of the 10 folds we define $\mathcal{D}_{-j} = \text{concat}(\{\mathcal{D}_i\}_{i \in \{1, \dots, 10\}, i \neq j})$. We then sample 12 models using cSGHMC on each \mathcal{D}_{-j} dataset. As before we get 120 models and for each fold \mathcal{D}_j we can use the held-out models, i.e. models trained on \mathcal{D}_{-j} , for distillation. Note that the dataset for distillation is the entire trainset, but for each data-point, we use only the predictions of 12 models that did not train on it.

Table 4: Comparison of ensemble techniques on STL-10, CIFAR-10, and CIFAR-100.

		STL-10			CIFAR-10			CIFAR-100		
		ACC (↑)	AGREEMENT	ECE (↓)	ACC (↑)	AGREEMENT	ECE (↓)	ACC (↑)	AGREEMENT	ECE (↓)
Bayesian	Train	100.0	98.22	2.99	99.96	91.85	6.38	99.94	97.53	4.15
	Test	81.85	87.85	2.17	94.41	86.08	5.56	77.79	71.97	3.07
	mixup	–	95.20	–	–	88.08	–	–	88.56	–
10 Fold	Train	96.95	89.47	12.45	99.99	97.78	1.77	99.97	94.08	4.77
	Held-out	76.67	91.86	1.42	93.72	93.42	1.21	74.52	78.95	3.67
	Test	80.48	80.45	5.85	94.84	91.75	1.48	77.70	72.81	2.43
	mixup	–	85.49	–	–	94.08	–	–	86.61	–
10 Bagging	Train	97.32	82.05	14.71	99.70	94.24	3.74	99.48	79.79	14.42
	Held-out	76.90	79.03	2.39	91.43	91.43	0.94	73.27	69.32	3.27
	Test	78.85	74.04	5.63	93.99	90.03	1.70	74.78	65.53	5.21
	mixup	–	78.01	–	–	90.83	–	–	73.59	–
120 Bagging	Train	96.33	77.84	18.85	99.99	94.63	3.59	99.98	79.97	14.08
	Held-out	77.79	71.85	8.59	93.85	91.69	0.81	74.68	69.13	3.77
	Test	77.77	70.49	8.57	94.13	91.09	1.12	75.16	67.68	4.02
	mixup	–	73.86	–	–	91.52	–	–	74.19	–

Table 5: Comparing FED + mixup and Out-Of-Bag ensembles on a held-out data. Test accuracy, agreement and ECE (%) on STL-10, CIFAR-10, and CIFAR-100.

		STL-10			CIFAR-10			CIFAR-100		
		ACC (↑)	AGREEMENT	ECE (↓)	ACC (↑)	AGREEMENT	ECE (↓)	ACC (↑)	AGREEMENT	ECE (↓)
Bayesian _{mixup}		80.94	97.16	2.55	93.68	93.71	0.78	74.56	88.20	2.07
10-Fold _{Held-out}		62.92	84.40	5.33	91.00	90.48	0.87	67.73	80.39	1.62
10-Bagging _{Held-out}		63.13	84.41	6.16	90.97	88.24	0.97	67.55	67.27	4.82
120-Bagging _{Held-out}		63.03	82.55	7.96	91.03	88.76	1.02	68.95	69.08	5.64

In bagging each bag samples N data points with repetition from a dataset of size N . We explore two alternatives, one is sampling 120 bags and sampling for each bag a single model using cSGHMC (named 120 Bagging), and the other is to sample 10 bags and from each to sample 12 models using cSGHMC (named 10 Bagging). The held-out dataset for distillation is constructed in the same fashion as described in the K-Fold alternative. The key difference is that for each data point, there is a different number of models that did not use it in training, due to the stochastic partitioning of bags.

Comparing these two approaches the K-fold has an advantage since each ensemble member was trained on exactly 90% of the training data while each ensemble member in bagging is trained on $\sim 66\%$. Bagging (with 120 bags) however has better diversity as when we distill we see a larger variety of ensemble model combinations.

Table 4 shows results for the Bayesian ensemble used throughout this paper and the method described in this section. As one can see the scores on the held-out datasets, is a good proxy for the test in terms of calibration, agreement, and accuracy (the lower score is due to only averaging a small number of ensemble models), but this comes in many cases at a price of reduced accuracy of the ensemble on the test set compared to the Bayesian ensemble.

Next, we distill the new ensembles using FED. We show the results of the distilled models using the held-out data, and compare them to our Bayesian ensemble distilled using the mixup dataset. As one can see from our results in Table 5, the Bayesian ensemble distilled using the mixup data is superior. We note that on all ensembles the best distillation results we achieved were by using only mixup, further proving the value of this augmentation scheme.

6 Conclusions

In this work, we present FED, a novel and general ensemble distillation approach. We show that this approach can distill ensembles while keeping desirable qualities such as accuracy, calibration, and diversity. This is done by maintaining the Bayesian approach of distribution over functions while mimicking the posterior with one that can be evaluated efficiently. Additionally, we show how the need for an auxiliary distillation dataset can be easily solved by using mix-up augmentation. Finally, our experiments show that FED achieves state-of-the-art results on various benchmarks in the domain of Ensemble distribution distillation. Our work doesn't bare negative societal impacts directly but can be exploited for negative impact by the practitioner.

References

- [1] Idan Achituve, Aviv Navon, Yochai Yemini, Gal Chechik, and Ethan Fetaya. Gp-Tree: A Gaussian process classifier for few-shot incremental learning. In *International Conference on Machine Learning*, pages 54–65. PMLR, 2021.
- [2] Idan Achituve, Aviv Shamsian, Aviv Navon, Gal Chechik, and Ethan Fetaya. Personalized federated learning with Gaussian processes. In *Neural Information Processing Systems (NeurIPS)*, 2021.
- [3] Leo Breiman. Random forests. *Mach. Learn.*, 2001.
- [4] Tom Brown, Benjamin Mann, Nick Ryder, Melanie Subbiah, Jared D Kaplan, Prafulla Dhariwal, Arvind Neelakantan, Pranav Shyam, Girish Sastry, Amanda Askell, et al. Language models are few-shot learners. *Advances in neural information processing systems*, 33:1877–1901, 2020.
- [5] Cristian Buciluă, Rich Caruana, and Alexandru Niculescu-Mizil. Model compression. In *Proceedings of the 12th ACM SIGKDD international conference on Knowledge discovery and data mining*, pages 535–541, 2006.
- [6] Olivier Chapelle, Jason Weston, Léon Bottou, and Vladimir Vapnik. Vicinal risk minimization. *Advances in neural information processing systems*, 13, 2000.
- [7] Adam Coates, Andrew Ng, and Honglak Lee. An analysis of single-layer networks in unsupervised feature learning. In *Proceedings of the fourteenth international conference on artificial intelligence and statistics*, pages 215–223. JMLR Workshop and Conference Proceedings, 2011.
- [8] Gal Cohen, Hayit Greenspan, and Jacob Goldberger. Learning probabilistic fusion of multilabel lesion contours. In *IEEE International Symposium on Biomedical Imaging, ISBI*, 2020.
- [9] Yufei Cui, Wuguannan Yao, Qiao Li, Antoni B Chan, and Chun Jason Xue. Accelerating Monte Carlo Bayesian prediction via approximating predictive uncertainty over the simplex. *IEEE transactions on neural networks and learning systems*, 2020.
- [10] Stefan Depeweg, Jose-Miguel Hernandez-Lobato, Finale Doshi-Velez, and Steffen Udluft. Decomposition of uncertainty in Bayesian deep learning for efficient and risk-sensitive learning. In *International Conference on Machine Learning*, pages 1184–1193. PMLR, 2018.
- [11] Ethan Fetaya, Yonatan Lifshitz, Elad Aaron, and Shai Gordin. Restoration of fragmentary babylonian texts using recurrent neural networks. *PNAS*, 2020.
- [12] Arthur Gretton, Karsten M. Borgwardt, Malte J. Rasch, Bernhard Schölkopf, and Alexander J. Smola. A kernel two-sample test. *J. Mach. Learn. Res.*, 13:723–773, 2012.
- [13] Chuan Guo, Geoff Pleiss, Yu Sun, and Kilian Q Weinberger. On calibration of modern neural networks. In *International Conference on Machine Learning*, pages 1321–1330. PMLR, 2017.
- [14] Kaiming He, Xiangyu Zhang, Shaoqing Ren, and Jian Sun. Deep residual learning for image recognition. In *Proceedings of the IEEE conference on computer vision and pattern recognition*, pages 770–778, 2016.
- [15] Geoffrey Hinton, Oriol Vinyals, Jeff Dean, et al. Distilling the knowledge in a neural network. *arXiv preprint arXiv:1503.02531*, 2(7), 2015.
- [16] Pavel Izmailov, Sharad Vikram, Matthew D Hoffman, and Andrew Gordon Gordon Wilson. What are Bayesian neural network posteriors really like? In *International Conference on Machine Learning*, pages 4629–4640. PMLR, 2021.
- [17] Alex Kendall and Yarin Gal. What uncertainties do we need in bayesian deep learning for computer vision? In *Neural Information Processing Systems (NeurIPS)*, 2017.
- [18] Diederik P Kingma and Jimmy Ba. Adam: A method for stochastic optimization. *arXiv preprint arXiv:1412.6980*, 2014.
- [19] Durk P Kingma, Tim Salimans, and Max Welling. Variational dropout and the local reparameterization trick. In *Neural Information Processing Systems (NeurIPS)*, 2015.
- [20] Anoop Korattikara Balan, Vivek Rathod, Kevin P Murphy, and Max Welling. Bayesian dark knowledge. *Advances in Neural Information Processing Systems*, 28, 2015.
- [21] Alex Krizhevsky, Geoffrey Hinton, et al. Learning multiple layers of features from tiny images. Technical report, University of Toronto, 2009.

- [22] Chun-Liang Li, Wei-Cheng Chang, Yu Cheng, Yiming Yang, and Barnabás Póczos. MMD GAN: towards deeper understanding of moment matching network. In *Neural Information Processing Systems (NeurIPS)*, 2017.
- [23] Yujia Li, Kevin Swersky, and Richard S. Zemel. Generative moment matching networks. In *International Conference on Machine Learning (ICML)*, volume 37, 2015.
- [24] Andrey Malinin and Mark Gales. Predictive uncertainty estimation via prior networks. *Advances in neural information processing systems*, 31, 2018.
- [25] Andrey Malinin, Bruno Mlodozeniec, and Mark Gales. Ensemble distribution distillation. In *International Conference on Learning Representations*, 2019.
- [26] David A. McAllester. Some pac-bayesian theorems. In *Conference on Computational Learning Theory (COLT)*, 1998.
- [27] Mahdi Pakdaman Naeini, Gregory Cooper, and Milos Hauskrecht. Obtaining well calibrated probabilities using bayesian binning. In *Twenty-Ninth AAAI Conference on Artificial Intelligence*, 2015.
- [28] Giung Nam, Jongmin Yoon, Yoonho Lee, and Juho Lee. Diversity matters when learning from ensembles. *Advances in neural information processing systems*, 34, 2021.
- [29] Radford M. Neal. MCMC using Hamiltonian dynamics. *Handbook of Markov Chain Monte Carlo*, 54:113–162, 2010.
- [30] Yuval Netzer, Tao Wang, Adam Coates, Alessandro Bissacco, Bo Wu, and Andrew Y Ng. Reading digits in natural images with unsupervised feature learning. 2011.
- [31] George Papamakarios. Distilling model knowledge. *arXiv preprint arXiv:1510.02437*, 2015.
- [32] Siyuan Qiao, Huiyu Wang, Chenxi Liu, Wei Shen, and Alan Yuille. Micro-batch training with batch-channel normalization and weight standardization. *arXiv preprint arXiv:1903.10520*, 2019.
- [33] Jake Snell and Richard Zemel. Bayesian few-shot classification with one-vs-each Pólya-Gamma augmented Gaussian processes. In *International Conference on Learning Representations*, 2020.
- [34] Yusuke Tashiro, Yang Song, and Stefano Ermon. Diversity can be transferred: Output diversification for white- and black-box attacks. In *Neural Information Processing Systems (NeurIPS)*, 2020.
- [35] Linh Tran, Bastiaan S Veeling, Kevin Roth, Jakub Swiatkowski, Joshua V Dillon, Jasper Snoek, Stephan Mandt, Tim Salimans, Sebastian Nowozin, and Rodolphe Jenatton. Hydra: Preserving ensemble diversity for model distillation. *arXiv preprint arXiv:2001.04694*, 2020.
- [36] Martin J. Wainwright. *High-Dimensional Statistics: A Non-Asymptotic Viewpoint*. Cambridge University Press, 2019.
- [37] Max Welling and Yee Whye Teh. Bayesian learning via stochastic gradient langevin dynamics. In *International Conference on Machine Learning (ICML)*, 2011.
- [38] Yeming Wen, Dustin Tran, and Jimmy Ba. Batchensemble: an alternative approach to efficient ensemble and lifelong learning. In *International Conference on Learning Representations (ICLR)*, 2020.
- [39] Jeremy HM Wong and Mark JF Gales. Multi-task ensembles with teacher-student training. In *2017 IEEE Automatic Speech Recognition and Understanding Workshop (ASRU)*, pages 84–90. IEEE, 2017.
- [40] Yuxin Wu and Kaiming He. Group normalization. In *Proceedings of the European conference on computer vision (ECCV)*, pages 3–19, 2018.
- [41] Jaesik Yoon, Taesup Kim, Ousmane Dia, Sungwoong Kim, Yoshua Bengio, and Sungjin Ahn. Bayesian model-agnostic meta-learning. *Advances in neural information processing systems*, 31, 2018.
- [42] Hongyi Zhang, Moustapha Cisse, Yann N Dauphin, and David Lopez-Paz. mixup: Beyond empirical risk minimization. In *International Conference on Learning Representations*, 2018.
- [43] Ruqi Zhang, Chunyuan Li, Jianyi Zhang, Changyou Chen, and Andrew Gordon Wilson. Cyclical stochastic gradient MCMC for Bayesian deep learning. In *International Conference on Learning Representations*, 2019.

A Implementation Details

Data. To keep experiments uniform, for all datasets (STL-10, CIFAR-10, and CIFAR-100) we used a train/val/test partitioning. The trainset and validset are constructed by a fixed split of 80%:20%.

Training details for baselines. In our experiments we compared FED with four baselines. (1) EnDD [25]. (2) EnDD + AUX [25]. (3) AMT [9]. (4) DM - Diversity-Matters [28]. (5) Hydra [35].

For all baselines we tried different learning rates [0.1, 0.01, 0.001] and batch sizes [32, 64, 100]. For EnDD and EnDD + AUX, we used the same temperature, temperature annealing, and optimizer that was used in the original paper. Training for 200 epochs for CIFAR-10, CIFAR-100, with and without AUX. Training for 400 epochs for STL-10 without AUX, and 200 epochs for STL-10 with AUX.

For AMT, we tried different alphas [1e1, 1e3, 1e5] and kept the rest as the original paper. For DM, due to high memory requirements, we were able to go up to a BatchEnsemble with an ensemble size of 8, while being able to use only batch size of 32. In addition, for this baseline we used a bigger memory GPU, unable to fit the training to our standard 11GB GPU used for the rest of our experiments.

For Hydra, due to high memory requirements, we were able to go up to a virtual ensemble size of 8, while being able to use only batch size of 32. Thus, our distilled model had 120 heads, but in training, at each iteration, we sampled randomly 8 heads and trained them. In addition, for this baseline with CIFAR-100 we used a bigger memory GPU, unable to fit the training to our standard 11GB GPU used for the rest of our experiments. Important to note that the distilled model is very heavy due to its 120 different heads, specifically, 3.95GB compared to 43.67MB Generator model for CIFAR-10.

The Mixup dataset. In the procedure of creating a Mixup [42] auxiliary dataset, we used a Beta distribution with $\alpha = 0.2$. In Mixup augmentation, and value $\lambda \in [0, 1]$ is sampled from a Beta distribution. λ is the interpolation coefficient $mixup - img = \lambda * img_1 + (1 - \lambda) * img_2$.

For STL-10, CIFAR-10, and CIFAR-100 datasets, we created 100k,150k,300k Mixup auxiliary datasets respectively.

Optimization of the Generator network. Generator training is done in the following setting: For the optimizer, Adam [18] optimizer with default parameters. For STL-10, CIFAR-10, and CIFAR-100 the best learning rate is 0.001 in the case of the Mixup auxiliary dataset. For the scheduler, we use MultiStepLR scheduler with milestones in epochs [35, 45, 55, 70, 80]. In each milestone multiplying the learning rate by a factor of 0.33. Memory limitations force us to use a virtual ensemble size equal to 8, which essentially means that in each iteration, we sample 8 probability vectors from the 120 probability vectors the auxiliary dataset contains for each example. We use batch size of 64. The combination of batch size = 64 and virtual ensemble size = 8 determines by the GPU memory capacity. We trained the generator for 200 epochs.

In addition, we set the std of the inserted noise to be a learnable parameter as part of the optimization. A value of 0.1 for std is used for initialization.

We share our code with detailed documentation and usage examples for reproducibility.

Experiments Environment. All experiments were done on NVIDIA GeForce RTX 2080 Ti with 11019MiB. For Hydra and DM baselines we had to use NVIDIA TITAN RTX with 24220MiB.

B Additional Experiments

B.1 Different Auxiliary datasets

As part of our research to find a suitable dataset for the distillation task, we compared several options. (1) Trainset - the dataset originally used for the ensemble training. (2) Validset - the held-out set during ensemble training, and now can be viewed as new unseen data (without gathering more unlabeled data). (3) Mixup - applying mixup augmentation on the trainset. We were guided by two important aspects. First, the data for the distillation task have to come from a source that does not rely on external or additional data. Second, the data needs to be easily created/generated.

B.1.1 Extended Ensemble Analysis

In table Table 6 we present an extended ensemble analysis of Accuracy, agreement, and calibration(ECE) over the different ensembles and different datasets.

Table 6: Ensemble analysis. Test accuracy, agreement & ECE (%) on STL-10, and CIFAR-10/100.

	STL-10			CIFAR-10			CIFAR-100		
	ACC (↑)	AGREEMENT	ECE (↓)	ACC (↑)	AGREEMENT	ECE (↓)	ACC (↑)	AGREEMENT	ECE (↓)
Train	100.0	98.23	2.99	99.97	91.85	6.38	99.95	97.53	4.15
Valid	81.20	87.77	3.17	94.91	86.08	6.18	78.31	70.67	4.38
Test	81.84	87.85	2.17	94.41	86.08	5.56	77.79	71.97	3.07
mixup	-	95.20	-	-	88.08	-	-	88.56	-

B.1.2 Generator with different auxiliary datasets

In the following Tables 7, 8, 9, and 10 we show results of training a Generator with different auxiliary datasets, over different ensembles - Bayesian, 10-Fold, 10-Bagging, and 120-Bagging respectively. In the Bayesian ensemble, the validset is a held-out set (20% of the entire dataset). For STL-10, CIFAR-10, and CIFAR-100 the validset is of size 1k, 10k, and 10k respectively. For 10-Fold, 10-Bagging, and 120-Bagging the held-out set is constructed as the entire trainset. But, each example uses for prediction only models in the ensemble that did not use this example in their training. This means that for the three ensemble alternatives, the held-out set is essentially the entire trainset using subsets of the ensemble. For STL-10, CIFAR-10, and CIFAR-100 the held-out size is 5k, 50k, and 50k respectively.

Results in Table 7 show that using our Mixup augmentation for auxiliary dataset yields the best accuracy and calibration. One observation is that the agreement of the generator trained with the validset is better. This is no surprise, the validset is essentially new unlabeled data that comes from the same distribution as the testset. While being better in terms of the agreement, the accuracy substantially decreases due to the small size of the validset. Thus, our main effort was indeed to find a method for creating more data that resembles the testset distribution, and we found Mixup as a good option.

Table 7: Ablation - FED with different auxiliary datasets on **Bayesian Ensemble**. Test accuracy, agreement & ECE (%) on STL-10, CIFAR-10, and CIFAR-100.

	STL-10			CIFAR-10			CIFAR-100		
	ACC (↑)	AGREEMENT	ECE (↓)	ACC (↑)	AGREEMENT	ECE (↓)	ACC (↑)	AGREEMENT	ECE (↓)
Trainset	65.06	97.18	5.00	92.58	99.16	1.92	68.34	97.58	9.61
Validset	53.31	94.07	6.30	82.64	83.60	3.47	54.13	87.17	1.43
Mixup	80.94	97.16	2.55	93.68	93.71	0.78	74.56	88.20	2.07

On 10-Fold 8, 10-Bagging 9, and 120-Bagging 10 the results share the same insights as on the Bayesian ensemble. In addition, thanks to the high diversity that comes from the ensemble itself, the distilled model also has a high diversity. In terms of accuracy, Mixup still has the upper hand. Furthermore, the held-out has a better agreement and better accuracy compared to the validset used in the Bayesian ensemble. A direction worth exploring in our opinion is to apply Mixup augmentation over the held-out set, thus, enjoying a large amount of unseen data.

Table 8: Ablation - FED with different auxiliary datasets on **10-Fold Ensemble**. Test accuracy, agreement & ECE (%) on STL-10, CIFAR-10, and CIFAR-100.

	STL-10			CIFAR-10			CIFAR-100		
	ACC (↑)	AGREEMENT	ECE (↓)	ACC (↑)	AGREEMENT	ECE (↓)	ACC (↑)	AGREEMENT	ECE (↓)
Trainset	64.51	97.65	8.75	91.04	94.73	4.82	66.43	86.43	10.72
Held-out	62.92	84.40	5.33	91.00	90.48	0.87	67.73	80.39	1.64
Mixup	77.32	97.25	9.65	93.84	94.10	0.99	74.99	84.51	1.62

Table 9: Ablation - FED with different auxiliary datasets on **10-Bagging Ensemble**. Test accuracy, agreement & ECE (%) on STL-10, CIFAR-10, and CIFAR-100.

	STL-10			CIFAR-10			CIFAR-100		
	ACC (↑)	AGREEMENT	ECE (↓)	ACC (↑)	AGREEMENT	ECE (↓)	ACC (↑)	AGREEMENT	ECE (↓)
Trainset	66.21	74.97	6.95	91.68	90.69	1.54	68.53	76.06	2.61
Held-out	63.13	84.41	6.16	90.97	88.24	0.97	67.55	67.27	4.82
Mixup	77.37	95.47	10.24	93.76	90.43	1.52	73.73	68.95	4.68

Table 10: Ablation - FED with different auxiliary datasets on **120-Bagging Ensemble**. Test accuracy, agreement & ECE (%) on STL-10, CIFAR-10, and CIFAR-100.

	STL-10			CIFAR-10			CIFAR-100		
	ACC (↑)	AGREEMENT	ECE (↓)	ACC (↑)	AGREEMENT	ECE (↓)	ACC (↑)	AGREEMENT	ECE (↓)
Trainset	63.50	76.03	8.91	91.26	90.92	2.15	69.12	76.88	2.95
Held-out	63.03	82.55	7.96	91.03	88.76	1.02	68.95	69.08	5.64
Mixup	76.34	95.64	13.91	93.54	90.84	0.97	74.26	72.53	3.22

C Performance

C.1 Runtime

We show in Figure 4 that for a wide range of batch sizes the runtime of our model scales approximately as $1 + (\# \text{ of } \epsilon \text{ samples})/35$ resulting in a considerable speedup. Specifically, the generator inference time with 120 epsilons takes 0.020 seconds, while ensemble inference time takes 4.075 seconds.

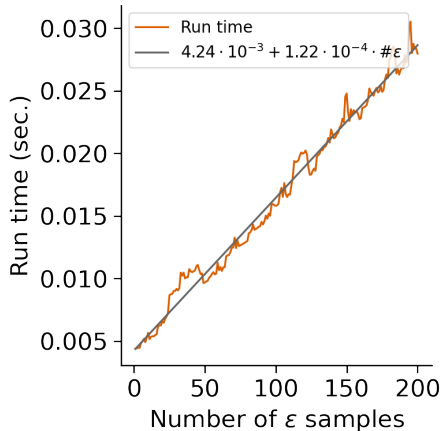


Figure 4: Runtime in seconds as a function of the number of ϵ s, i.e batch size.

C.2 Memory

For STL-10 and CIFAR-10, the memory requirement of the entire ensemble is 5.117GB, i.e 120 models of ResNet-18 that each requires 43.669MB.

Our generator, which essentially is almost a regular ResNet-18, requires 43.677MB.

For CIFAR-100, the memory requirement of the entire ensemble is 5.261GB, i.e 120 models of ResNet-18 that each requires 43.849MB.

Our generator, which essentially is almost a regular ResNet-18, requires 43.858MB.

D Dirichlet goodness of fit

Few of our baselines consider the task of distillation as learning the Dirichlet distribution over the prediction for every input example. We argue that the Dirichlet distribution imposes a limitation on

Table 11: Dirichlet distribution fitness test.

	STL-10 AGREEMENT	CIFAR-10 AGREEMENT	CIFAR-100 AGREEMENT
Ensemble	87.85	86.08	71.97
Dirichlet	91.01	90.66	77.06

the expressive power of the distilled model. Thus, introduces an irreducible error in the distilled model. In order to show that, we test how well the Dirichlet distribution fits the probability vectors that the ensemble produces.

In the following experiment, we take each example from the testset, and perform an MLE procedure to find the Dirichlet distribution that most likely produces those probability vectors $\{p(y_*|\mathbf{x}_*, \theta_1), \dots, p(y_*|\mathbf{x}_*, \theta_M)\}$. Next, we test the Agreement metric introduced in Section 5 over probability vectors sampled from the computed Dirichlet distribution, i.e $\{y_i\}_{i=1}^M \sim \text{Dirichlet}(\text{alphas})$. Suppose the Dirichlet distribution expressiveness is good enough, we would expect a perfect match to the predictive distribution of the ensemble on this example.

Results in Table 11 suggest that indeed, there is a gap between the predictive distribution of the ensemble and the maximum likelihood Dirichlet distribution in terms of the agreement. For all three datasets, the agreement of the ensemble over the testset is lower (higher diversity) than the agreement of the Dirichlet distribution over the testset. This means, that leaning on a Dirichlet-based distilled model has a fundamental limitation.